Low Temperature Photoluminescence Study in GaAs Quantum Well Heterostructure

PH4201
Spring 2017

Submitted by
Abhijeet Kumar
13MS027

Supervisor
Dr. Bipul Pal

May 1, 2017

Contents

Abstract

The mechanism for low-temperature photoluminescence emissions in $GaAs-Al_xGa_{1-x}As$ single quantum well heterostructure is studied in details using PL spectroscopy as a function of temperature and laser excitation intensity. PL peak intensity varies linearly with the excitation power and decreases with increasing temperature, exhibiting a small redshift. Band gap of the sample shows temperature dependence and behaves like a typical semiconductor. The variation of band gap against temperature is an important characteristic of the semiconductor and can be explained both theoretically and analytically using a modified version of Varshni equation. Importance of excitons in PL spectra at low temperature is observed.

Chapter 1

Introduction

Spectroscopy is a tool to study the interaction between radiation and matter as well as to gain insight into the electronic structure of the matter. In spectroscopy, frequency and intensity of a radiation is analysed after it gets reflected, emitted or observed by a matter. Spectroscopic investigations can be performed over a wide range of frequency and hence it has several applications into modern science e.g. investigation of electronic structure of matter (by photon emission or absorption), phonons (Raman spectroscopy), crystal structure (X-ray diffraction), atomic and molecular structure investigation (NMR spectroscopy) *etc.*

Luminescence is a phenomena in which radiation is emitted by a material when electrons make transition from excited state to ground state within the system. In **Photoluminescence**, the excitation of electrons occurs due to absorption of photons. Light is directed onto a sample where it is observed and a process called *photo-excitation* occurs, where the system gets excess energy.

Due to photo-excitation electrons within the material jump to the higher permissible excited states. Eventually, these electrons return back to their equilibrium state and the excess energy is released in form of light. The spectrum of this light gives information about the electronic structure and other properties of the material.

In this project, we study the photoluminescence in single quantum well heterostructure of a direct band gap semiconductor Gallium Arsenide (GaAs). Detailed physics associated with the photoluminescence process inside a semiconductor is explained in next chapter. In chapter 3, detailed description of experimental set-up is presented. Observations and analysis of results upon performing the experiment are discussed in chapter 4. We finally conclude the report by proposing our next step for future work.

Chapter 2

Fundamentals

2.1 Light-matter interaction

Semi classical approach is used to understand the light matter interaction phenomenon, in which light is treated as classical EM wave and electrons are treated quantum mechanically. For an electron inside electromagnetic field, the Hamiltonian includes certain interaction terms which are treated by time-dependent perturbation theory [1]. The momentum $\hat{p}$ which corresponds to unperturbed Hamiltonian $\hat{H}_0$ changes to $\hat{p}+e\hat{A}$ under the effect of perturbation term H' with $\hat{A}$ being the vector potential. This yields

$$\hat{H} = \frac{1}{2m}(\hat{p} + 2\hat{A})^2 + \hat{V}(r) = \hat{H}_0 + H' \tag{2.1}$$

with $$\hat{H}_0 = \frac{\hat{p}^2}{2m} + \hat{V}(r) \quad \text{and} \quad \hat{H}' = \frac{e}{2m}\hat{p}.\hat{A}$$

Transition rate describing the probability of transition from state ψ_m to ψ_n (*Fermi's golden rule*) is given by

$$W_{m\to n} = \frac{2\pi}{\hbar}|\hat{M}'_{nm}|^2\delta(E_n - E_m - \hbar\omega) \tag{2.2}$$

where $|\hat{M}'_{nm}|$ is the matrix element given by

$$|\hat{M}'_{nm}| = \langle\psi_n|\hat{H}'|\psi_m\rangle = \int \psi_n^*\hat{H}'(r)\psi_m^* \tag{2.3}$$

Thus the transition between the discrete energy levels m and n occurs when $|E_n - E_m| = \hbar\omega$. Also, $\triangle m = 0$, ± 1 and $\triangle l = \pm 1$ need to be obeyed, where m and l are quantum numbers.

2.2 Photoluminescence in semiconductors

Inside a semiconductor (more generally a solid), the discrete energy levels m, n turn into continuous energy bands. These are no longer discrete. Therefore a

different process occurs, controlling the light-matter interaction inside semiconductors. The delta function from (2) gets replaced by DOS (density of state) inside a solid, while the matrix element get replaced by Bloch's wave function. We need not go deep into the band structure inside semiconductors. Photoluminescence process inside semiconductors is explained in following sections.

2.2.1 Semiconductors

In semiconductors, there is a finite band gap (E_G) between the conduction band (CB) and valance band (VB). Based on the band structure, there are two types to semiconductors, namely *direct band gap* semiconductors and *indirect band gap* semiconductors. In direct band gap semiconductors such as GaAs, the minimum of conduction band and maximum of valance band lie at the same point $k = 0$ in the momentum space, while in indirect band gap semiconductors, these two points don't lie at $k = 0$ (figure 2.1).

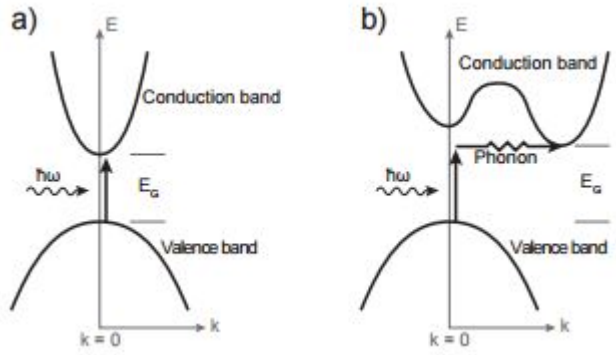

Figure 2.1: a) Direct band gap semiconductor, b) Indirect band gap semiconductor [2].

In order to have an optically induced inter band transition of charge carriers (electrons and holes), *energy* and *crystal momentum* conservation is required. In direct band gap semiconductors, the only critical requirement is the conservation of energy $E_G = \hbar\omega_{photon}$. Optical transition of electrons from valance band to conduction band gets possible for $\hbar\omega_{photon} > E_G$. For indirect band gap semiconductors, a phonon helps in maintaining crystal momentum conservation.

2.2.2 Energy transfer

The optical transition of electrons from the conduction band to the valance band follows by a series of events leading to energy transfer (figure 2.2) [4]. The photo-excitation creates a non equilibrium population of free carriers (electrons

in CB and holes in VB).
This non equilibrium population of free carriers spreads out in k-space through *carrier-carrier scattering*. This involves electron-electron scattering, hole-hole scattering and electron-hole scattering. Through multiple scattering, free carriers get internally thermalized and the energy gets redistributed among them without changing the total energy. This process occurs at a time-scale of few femtoseconds.

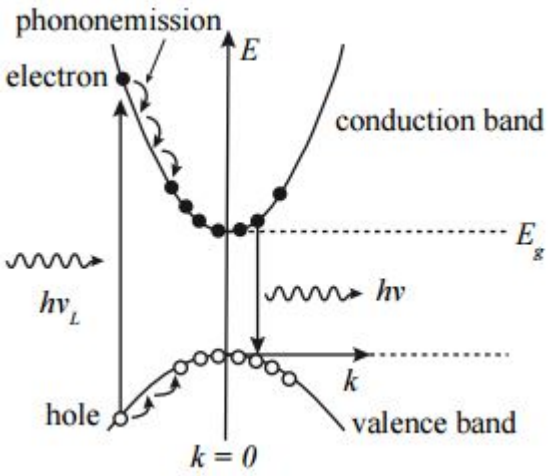

Figure 2.2: Overall process of photoluminescence in semiconductors. Here is an example of radiative recombination [2].

This is followed by *carrier-phonon scattering* through which energy is transferred from excited electrons to the crystal. This is a bit slow process due to poor electron-phonon coupling (time order of few picoseconds). These two processes however, don't change the free-carrier density, which is taken care of by *carrier-recombination* and *diffusion* process.
Following the electron-phonon scattering, the electron makes transition back to VB and *recombines* with a hole, hence decreasing the free carrier density in momentum space. On the other hand, carrier-diffusion refers to the average motion of free carriers from high density region to low density region, thereby redistributing the density. Time order for this process is of picoseconds.
There are mainly two kinds of recombination process, namely *radiative* recombination and *non radiative* or *Auger* recombination. In radiative recombination, there occurs a spontaneous emission of photons, while, in non radiative recombination, the transition energy gets transferred to another free carrier and hence the lattice. The radiative recombination rate is proportional to the product of electron-density in CB (n) and hole-density in VB (p).

2.3 Excitons

We have seen that photoluminescence is the result of radiative recombination of electron-hole pair. Excitons are the electron-hole pair which are bound together by electrostatic interaction. These are unstable against the electron-hole recombination, but often dominate the absorption spectrum just below the band edge. When the electron-hole pair is created by absorption of photon, the absorption spectrum contains sharp lines just below the band gap (figure 2.3). These sharp lines are due to excitons.

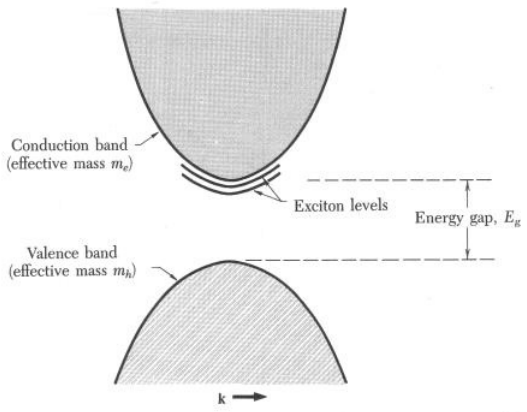

Figure 2.3: Exciton bands below the conduction band inside a semiconductor [18].

Excitons play important role in determining optical properties of semiconductors. They are mostly observable at low temperature due to the limitations of its binding energy. For stable excitons, binding energy needs to be less than thermal energy.

2.4 Quantum wells

Quantum wells are thin layered semiconductor structures in which one thin semiconductor "well" layer (where electrons and holes are confined) is sandwiched between two other semiconductor "barrier" layers. Quantum confinement of the charge careers (electrons and holes) derive the their special properties. Basic understanding of quantum wells comes from the quantum mechanical study of "a particle in a box" model.
Excitons play very important role inside quantum wells. Unlike the transition of electrons or holes in between valance and conduction band inside a semiconductor, we consider the creation of electron-hole pair and deal with them. It is

possible to create an exciton with an energy E_B less than that required to create a "free" electron-hole pair. The energy required to create this free pair is actually the simple band gap energy E_G of a semiconductor ($E_{excitons} = E_G - E_B$). This is the reason why we expect some optical absorption at photon energies just below the band-gap energy. Also, because electrons and holes are confined within the thin layer, their size is very small and they have large binding energy. Due to this they orbit faster, consequently, they complete a classical orbit before being destroyed by optical phonon, hence maintaining resonance.

2.5 Optical transition in semiconductors

From (2.1), we can obtain the transition rate of free careers inside a semiconductor. Considering that the state m is completely occupied and state n is completely empty, the upward transition rate of electrons per unit volume inside a crystal is given by

$$R_{m\to n} = \frac{2}{V}\sum_{k_m}\sum_{k_n}\frac{2\pi}{\bar{h}}|\hat{M}'_{nm}|^2\delta(E_n - E_m - \hbar\omega)f_m(1-f_n) \tag{2.4}$$

where the Fermi-Dirac equation

$$f_m = \frac{1}{1+e^{(\frac{E_m - E_n}{k_b T})}} \tag{2.5}$$

is the probability that the state m is occupied. Similarly, $(1-f_n)$ shows the probability that the state n is empty [3].
Similarly, total downward transition rate per unit volume can be written as

$$R_{n\to m} = \frac{2}{V}\sum_{k_m}\sum_{k_n}\frac{2\pi}{\bar{h}}|\hat{M}'_{mn}|^2\delta(E_m - E_n - \hbar\omega)f_n(1-f_m) \tag{2.6}$$

So, the net upwards transition rate per unit volume becomes

$$R = R_{m\to n} - R_{n\to m} = \frac{2}{V}\sum_{k_m}\sum_{k_n}\frac{2\pi}{\bar{h}}|\hat{M}'_{nm}|^2\delta(E_n - E_m)(f_m - f_n) \tag{2.7}$$

Optical absorption coefficient α which is the ratio of number of photons absorbed (per unit volume per unit second) and number of photons injected (per unit area per unit second) is calculated to be

$$\alpha(\hbar\omega) = C_0\frac{2}{V}\sum_{k_m}\sum_{k_n}\langle n|e^{ik.r}\hat{e}.\mathbf{p}|m\rangle\delta(E_n - E_m - \hbar\omega)(f_m - f_n) \tag{2.8}$$

$$\text{where } C_0 = \frac{\pi e^2}{n_r c\epsilon_0 m_0^2\omega}$$

For the case of quantum wells, calculation of the optical transition matrix is done in a different way, which we do not go in details here.

Chapter 3

Instrumentation

In the previous chapter, we studied the physics behind photoluminescence process in semiconductors. We will now discuss the experimental components and design in details.

The experiment basically requires a sample, a light source, an optical arrangement and detector. The sample (kept inside cryostat) is excited as the light coming out of the source is focused on the it using a lens. An excited sample radiates photons in form of light which is again focused at the entrance slit of a monochromator. The monochromator uses grating technique to separate light into narrow wavelength bands such that only the desired wavelength band of light passes through the exit slit and is detected by Photo Multiplier Tube that enhances the light signal. A lock-in amplifier is used to reduce signal to noise ratio from the detected signal, and it reads the signal caused by photoluminescence only. Thus we get the photluminescence spectrum as a variation of output light intensity with respect to input photon energy.A pictorial representation of set up is shown in figure 3.1.

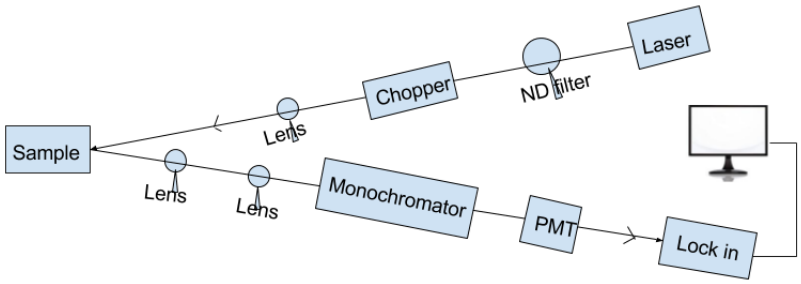

Figure 3.1: Schematic diagram of instrument set up.

3.1 Sample arrangement

The sample used for photoluminescence in this experiment is a $GaAs - Al_xGa_{1-x}As$ single QW heterostructure. GaAs is a direct band gap semiconductor with E_G value 1.42 eV at $T = 300$ K.
Since, in this experiment low temperature PL is being observed, the sample is kept inside a *cryostat*. The temperature inside cryostat is cooled upto $T = 4.2$ K and temperature variation is controlled using liquid Helium and a heater. Vacuum is also being maintained around the sample.
Light coming out of semiconductor laser gets access to the sample through a glass window in cryostat. This light intensity is usually very high, so we use neutral density filter to reduce its intensity upto desired value.

3.2 Monochromator

The light emitted from the sample, is helped by a simple lens arrangement to fall at the entrance slit of the monochromator (fiure 3.2). A monochromator consists of thin slits, concave mirrors and a diffraction grating. The incident light gets collimated by the concave mirror, falls on the diffraction grating and is reflected towards a second concave mirror at the other extreme which in turn focuses the light on the exit slit.

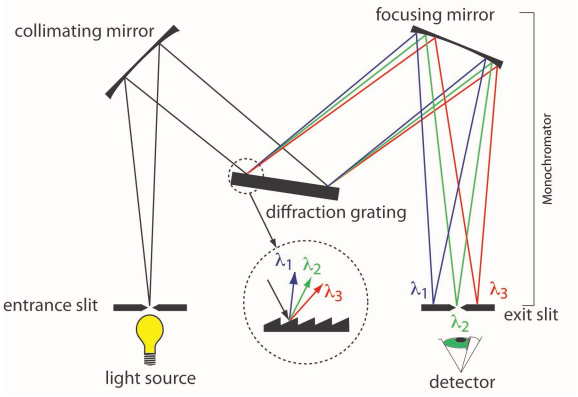

Figure 3.2: Schematic diagram of a monochromator in function [15].

The design of the diffraction grating is such that when the light falls on it, it reflects different wavelength of light at different angles, thus spreading out the light in narrow bands of wavelength. This light falls on the second mirror, which reflects it in a manner to focus a single narrow wavelength band of light to the exit slit. Hence, only light of a particular wavelength band can pass through the slit, no others.

Thus the monochromator allows scanning over a range of wavelength and letting corresponding light signal pass through.

3.3 Photo Multiplier Tube

The Photo Multiplier Tube (PMT) is placed next to the monochromator and it detects the signal coming out of the monochromator and amplifies it (this signal is very weak). PMT is a current device and it produces current proportional to the incident light intensity.

PMT is a vacuum tube which contains a photoathode, a series of dynodes and an anode (figure 3.3). The incident light falls on the photovcathode, which emits photoelectrons by photoelectric effect. These photoelectrons are accelerated (a voltage gradient between photocathode and dynodes leads to the acceleration) and focused on first dynode. The electrons strike the surface and emit more secondary electrons. These secondary electrons are again accelerated towards the second dynode and so on. Photo electrons ejected by the last dynode is collected at the anode as a current pulse. The strength of the pulse depends on the voltage applied to the PMT, which is controllable. A higher voltage result in large pulse. In our experiment, PMT voltage is set to 1000 V.

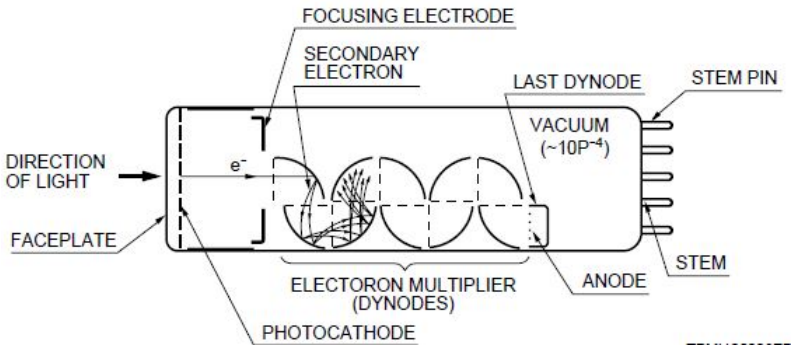

Figure 3.3: Photo Multiplier Tube [16].

The amplified signal coming out of PMT contains quite a bit amount of noise that needs to be dealt with using lock-in amplifier.

3.4 Lock-in amplifier

Lock-in amplifiers detect and measure very small AC signals by reducing the signal to noise ratio. Lock-in works on phase-sensitive detection (PSD) technique.

It has very narrow band-pass, so it allows the signal with specific reference frequency and phase to pass, and blocks the signals with frequencies other than the reference frequency (i.e. noise). Lock-in has four main components: input signal (a sine wave with frequency ω_{sig}), reference signal (provided either externally or created by lock-in itself; frequency ω_{ref}), DC amplifier and low-pass filter.

Lock-in amplifies the input signal and multiplies it with the reference signal (in our set up, the reference signal is a sine wave created by lock-in itself). The output of their product consists of a phase term relating ω_{sig} and ω_{ref} (3.2). The low-pass filter only detects the signals with ω_{ref} very close to ω_{sig}, hence removing the noise signal at frequencies far from ω_{ref}. Noise at frequencies close to ω_{ref} can be rejected by using narrow low pass filter bandwidth. The signal at ω_{sig} equal to ω_{ref} gives true DC output, the desired signal for measurement (3.3). Basic function of lock in is demonstrated by the following example [17].

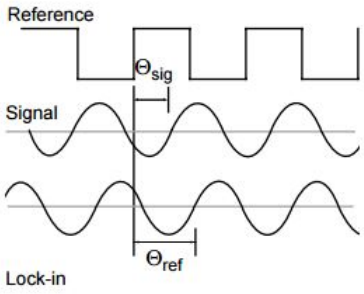

Figure 3.4: Lock in signal representation [17].

In figure 3.4, there is a reference signal in square wave form at frequency ω_r. This signal when excites the experiment, the response is the signal waveform of the form $V_{sig}(\sin\omega_r t + \theta_{sig})$ where V_{sig} and θ_{sig} are signal amplitude and phase respectively. The lock in generates its own internal reference signal $V_L(\sin\omega_L t + \theta_{ref})$.
The output of the PSD is the product of two Sine waves and is given by

$$V_{PSD} = V_{sig}V_L \sin(\omega_r t + \theta_{sig}) \sin(\omega_L t + \theta_{ref}) \tag{3.1}$$

$$or, \quad V_{PSD} = \frac{1}{2}V_{sig}V_L \cos([\omega_r - \omega_L]t + \theta_{sig} - \theta_{ref}) \tag{3.2}$$

$$-\tfrac{1}{2}V_{sig}V_L \cos([\omega_r + \omega_L]t + \theta_{sig} + \theta_{ref})$$

When this signal passes through low pass filter with $\omega_r = \omega_L$, we get the desired DC signal output

$$V_{PSD} = \frac{1}{2} V_{sig} V_L \cos(\theta_{sig} - \theta_{ref}) \tag{3.3}$$

One important thing to notice is that the signal frequency ω_{sig} must be set to one fixed value in order to be accurately detectable by the lock in. As an AC signal has a fixed frequency, therefore, in our experiment, we have used a chopper circuit to make the original DC laser signal behave like an AC one, before it falls on the sample.

3.5 Software designation

After lock-in gives us the desired signal output, we get the data for obtaining PL spectrum. But it is not very simple to extract the measurements from the lock-in and to obtain the spectrum. This is because the measurement needs to be done over a range of incident wavelength and needs to be repeated at each wavelength for better accuracy of the experiment, which is not possible to maintain manually. For example, in our experiment, we scanned over the incident photon wavelength range 790 nm to 810 nm with step size 0.1 nm and at each successive wavelength value, 100 measurements were taken and averaged out.

In order to perform this task, LabVIEW programming was used. LabVIEW is a computer program, which basically connects the instrument virtually to the computer. It reads the response of the instrument and stores them into the computer. In our experiment, two important measurements need to be taken care of. Firstly, the incident photon wavelength, which the monochromator reads and the second one is the PL signal which is ultimately measured by lock-in. A LabVIEW program is written using various commands such that it reads the photon wavelength form the monochromator and PL signal from the lock-in, writes these data into a *.txt* file and stores the file into the computer. Note that the LabVIEW program reads hundred values of PL signal for one particular wavelength and averages them out before writing them into the *.txt* file. The LabVIEW program also measures the lock-in phase, which is not of any experimental use though.

Thus we get the data for our desired experiment, which gives us a photoluminescence spectrum. It is to be noted that the experimental set up for this experiment is very critical. There are various challenges before us while setting up the experiment. The light source, sample and detector alignment needs to be perfect so that the maximum amount of light strikes the sample, and upon emission, maximum amount of signal is detected. We need to be careful as we are working with laser. The experiment should be carried in dark in order to avoid background noise because PMT is very sensitive and it may give extra noise when some background light is present.

Chapter 4

Observations

We saw in the previous chapter that setting up the experiment is an important part of carrying out the whole experiment. After the set up is done as perfect as it could be, next part of job is to collect data. Maintaining a constant background inside the laboratory (to avoid background noise), light source is turned on and the light is allowed to fall on the sample. Sample in response exhibits pholuminescence. The emitted photons pass through the monochromator and then get detected by PMT. The amplified signal from PMT enters lock-in amplifier which removes the noise and detects the original photoluminescence signal emitted by the sample. Using the LabVIEW program, the data are stored in a *.txt* file. Another software, named *origin* is used to plot the data and obtain the corresponding PL spectrum.

In our experiment, two important aspects of PL has been studied, as are discussed below.

4.1 Power dependence of photoluminescence

In power dependent measurement, temperature around the sample is fixed at $T = 4.2\ K$ and PL spectrum is obtained for different magnitude of laser power (varied between 0.460 mW to 0.001 mW) [figure 4.1]. We were not able to obtain the PL spectrum for laser power below 0.001 mW due to set up limitation and a weak response by monochromator due to presence of white light (background).

Analysis:
The PL spectrum peak is proportional to the laser power and varies linearly with it, also consistent with figure 4.2. The PL signal reaches as high as 140 mV (for laser power 0.460 mW) and as low as 0.5 mV (for laser power 0.001 mW). High laser power injects more number of photons to the sample which in turn causes higher output signal by radiative recombination of electrons and holes [10]. At low laser power, the rate of radiative recombination is less and it

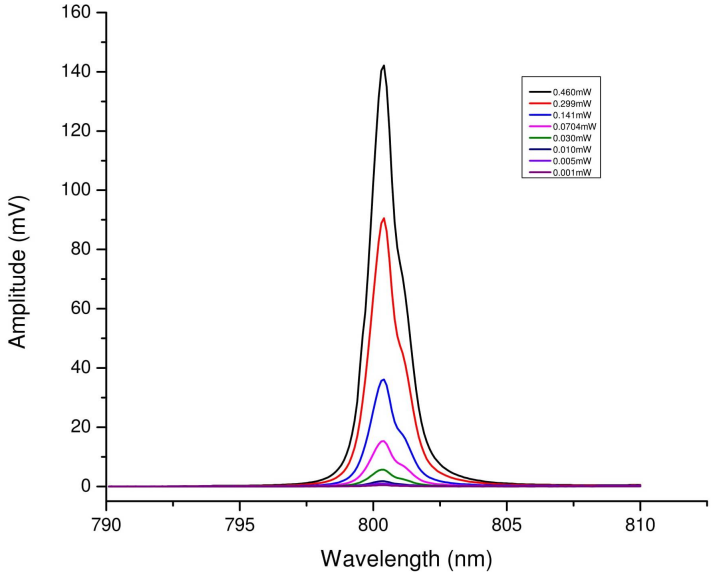

Figure 4.1: PL spectrum at $T = 4.2\ K$.

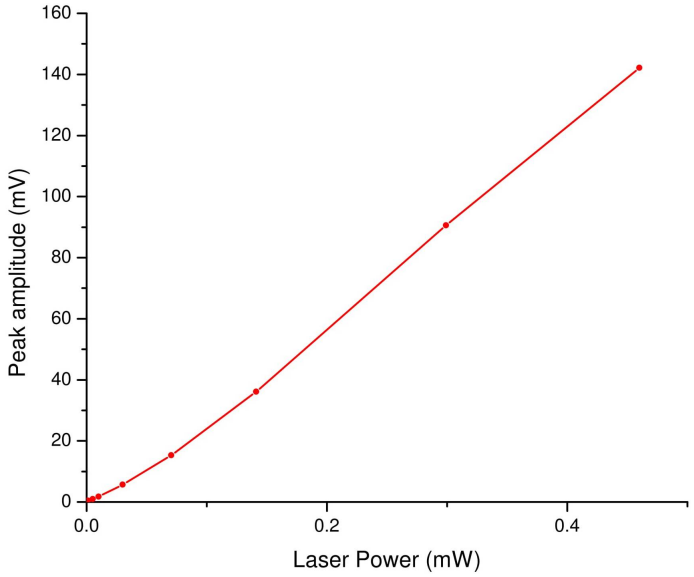

Figure 4.2: PL peak voltage vs laser power.

increases with increase in excitation power, as the careers get pumped. Therefore we get linear relationship between PL peak amplitude and laser power. Sometimes, at higher excitation power, when all the localized states (finite in number) get filled, it allows other excitons to become free and subsequently, recombine non radiatively [11]. However, this does not happen in this case. The peak wavelength for the sample (here 801.3 nm) remains independent of the laser power. This indicates that the laser power doesn't affect the band gap of GaAs QW.

4.2 Temperature dependence of photoluminescence

Output power of the laser is kept at 0.141 mW, while the temperature around the sample is varied from 4.2 K to 100 K. Photoluminescence spectrum is obtained for each set of parameters (figure 4.3).

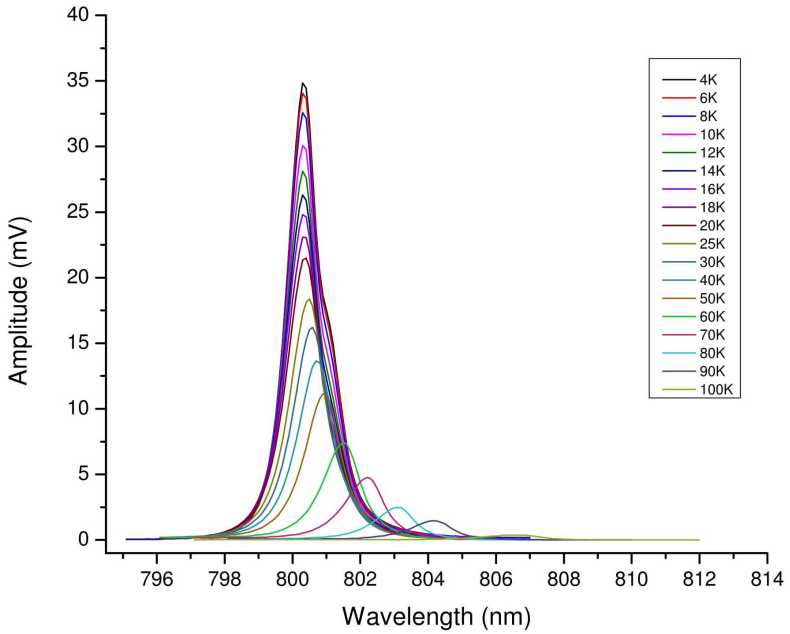

Figure 4.3: Temperature dependent PL spectrum at laser power 0.141 mW.

Analysis:
As the temperature increases, the PL spectrum peak decreases (figure 4.4) and

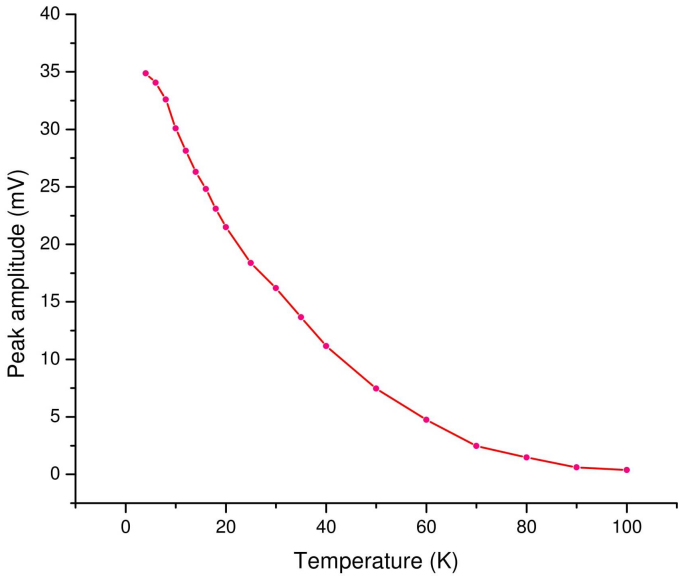

Figure 4.4: PL peak voltage vs Temperature.

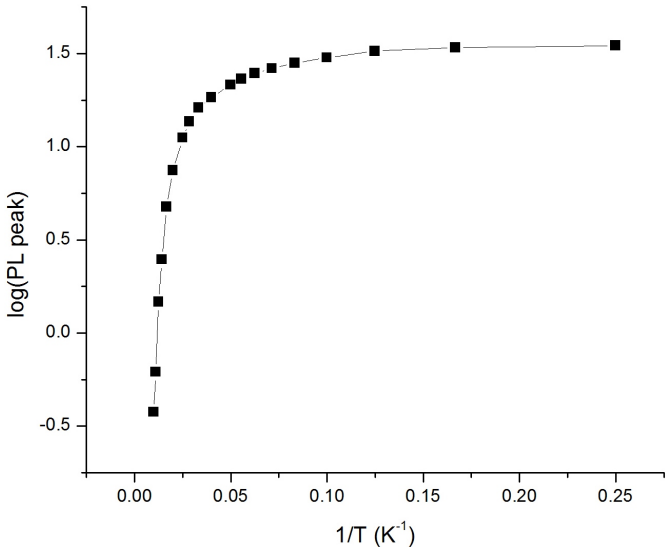

Figure 4.5: log of PL peak voltage vs 1/Temperature.

shifts towards higher wavelength (redshift). Excitons have certain binding energy (ranging from 1 meV to 1000 meV). So, as the surrounding temperature

increases, the thermal energy also increases and eventually leads to excitonic dissociation. Therefore, at higher temperature, the PL peak intensity decreases and redshift occurs. At lower temperature, the dissociation of excitons will decrease, hence we would observe higher PL peak intensity.

The decrease in PL intensity with temperature can be seen as a competition between radiative and non radiative recombination process. At low temperature, careers are localized [14] and recombining radiatively. Increasing temperature leads to thermally activated non radiative recombination, which is characterized by an activation energy. From the log plot in figure 4.5, it is observed that in low temperature region, the PL intensity remains constant. At higher temperature, it follows a straight line (characteristic of an exponential relation). In the intermediate region, it decreases, but not exponentially. This plot can be fit using the Arrhenius formula [9,12,13]

$$I(t) = \frac{I_0}{1 + ae^{-}E_a/kT} \tag{4.1}$$

where I_0 is the Pl intensity at zero temperature, a is the ratio of radiative and non-radiative career lifetime and E_a is the activation energy for non radiative recombination.
The (FWHM) full width at half maximum increases with temperature. This happens due to the morphology of band structures. Due to fluctuations of the thickness of GaAs QW layer across lateral direction, the effective band gap in GaAs QW has a shape as in figure 4.6 [9].
A better understanding of temperature dependence of PL can be achieved by understanding the corresponding band gap variation.

4.3 Band gap variation with temperature

From the temperature dependence of PL data, band gap energy E_G corresponding to each wavelength can be obtained.

$$E_G = h\nu = \frac{hc}{\lambda} \tag{4.2}$$

$$or, \quad E_G = \frac{1240}{\lambda(nm)} eV \tag{4.3}$$

Figure 4.7a shows band gap variation against temperature ranging from 4 K to 100 K. It can be seen that the decrease in band gap E_G is very small for temperature from 4 k to 20 K, whereas from 20 K to 100 K, it decreases more rapidly. This can be explained by the previous argument of excitonic binding energy. At temperature below, 20 K, their binding energy remains higher than the thermal energy. This leads to their stronger association and hence has very little affect on the band gap E_G.

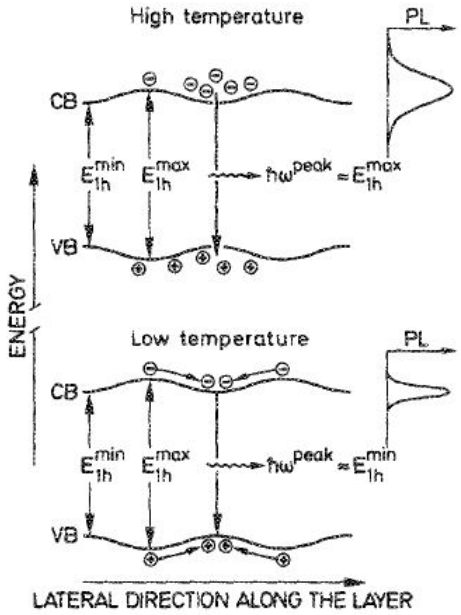

Figure 4.6: Band structure in Quantum Wells due to lateral thickness fluctuations.

However, The variation is not linear throughout. In a typical semiconductor, temperature dependence of band gap depends on the lattice parameter and electron-phonon coupling [8]. As the temperature increases, atomic vibration due to thermal energy increases so that the inter atomic spacing also increases. This decreases the potential felt by an electron, which in turn reduces the band gap. It is the electron-phonon coupling though, which dominates the behaviour of band gap.

4.3.1 Varshni equation

Varshni equation [6] is widely accepted relation to describe temperature dependence of band gap in semiconductors.

$$E_G(T) = E_g(0) - \frac{\alpha T^2}{(T+\beta)} \tag{4.4}$$

where $E_g(0)$ is the band gap of semiconductor at zero temperature and α and β are fitting parameters characteristic to particular material, β being related to the Debye temperature associated with phonons.
It gives a good fit to the band gap vs temperature plot. Unfortunately, it has

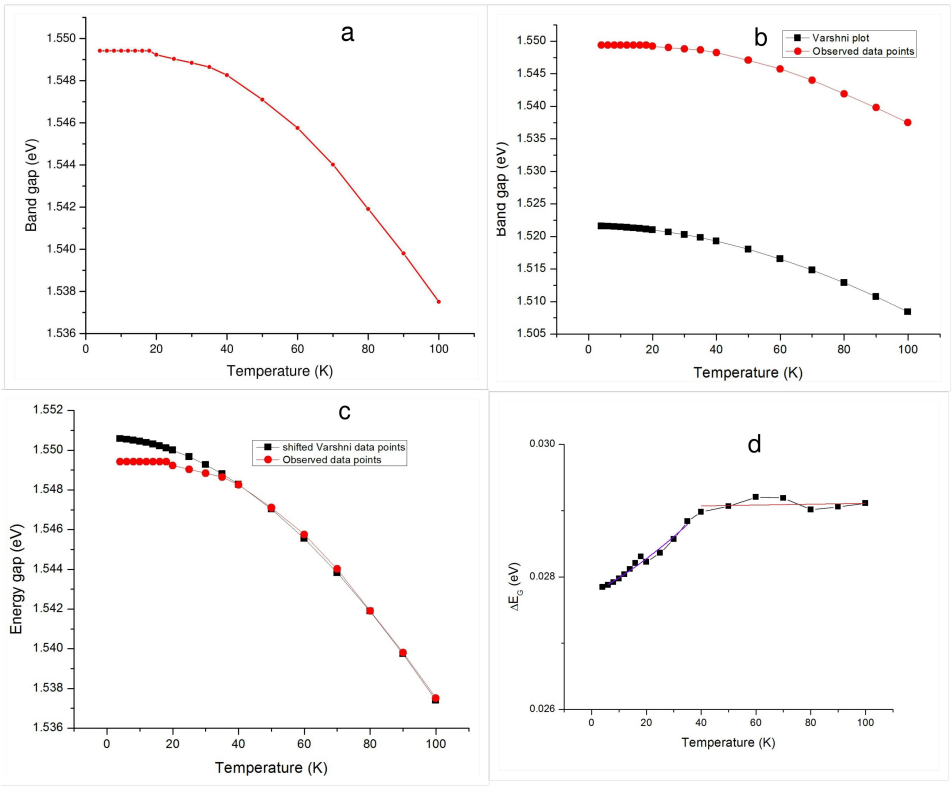

Figure 4.7: Band gap in GaAs QW vs Temperature at laser power 0.141 mW.

certain theoretical limitations as β sometimes possesses negative value. Also, at low temperature, where the temperature dependence of E_g is very weak (almost independent), Varshni relation doesn't give a proper fit as it predicts a quadratic relation at low temperature.
Many attempts have been made to modify the Varshni equation. A replacement equation for the Varshni equation was proposed by O'Donnell *et al.*[7] given by

$$E_G(T) = E_g(0) - S\langle\hbar\omega\rangle[coth(\langle\hbar\omega\rangle/2kT) - 1] \tag{4.5}$$

where S is dimensionless electron-phonon coupling term and $\langle\hbar\omega\rangle$ is the average phonon energy.
This equation fits the band gap curve nicely at both high and low temperature. At high temperature:

$$kT \gg \langle\hbar\omega\rangle \Rightarrow E_G(T) = E_g(0) - 2SkT \tag{4.6}$$

so that the slope $(\frac{dE_G}{dT})_{max} = -2Sk$ (linearly decrease) and

At low temperature:
$kT \ll \langle \hbar\omega \rangle$, so, $E_G(T) \cong E_g(0)$ (independent of temperature)—exactly what is expected theoretically.

4.4 Plots comparison

Figure 4.7 represents the comparison between the plot observed during experiment and the one expected from Varshni equation (using fitting parameters). Actually, we compare the observed band gap with the band gap of bilk GaAs. This is shown in figure 4.7*b*. We see that the behaviour of band gap is similar for GaAs bulk and QW, with a narrow difference in magnitude ($0.029\ eV$). We shift the data points obtained using Varshni equation to coincide it with the observed data points (figure 4.7*c*). It is observed that at temperature above $30\ K$, Varshni equation fits the observed plot quite nicely. At low temperature though, Varshni data points show non linearity and thus do not fit the plot correctly. This deviation can be justified from our earlier discussion that Varshni equation do not satisfy the behaviour at low temperature [6]. The difference between GaAs bulk and GaAs QW band gap against temperature is plotted in figure 4.7*d*. This plotted is fitted with quadratic function at low temperature (below $40\ K$) and is consistent with Varshni equation, according to which at low temperature the band gap varies as T^2. At higher temperature too, it is consistent with Varshni equation as we find the energy difference to be almost constant. Thus we that the band gap variation of GaAs QW bahaves very similar to that of GaAs bulk. Also, it justifies the Varshni equation.

We also tried to compare the observed data with the equation proposed by O'Donnell. From the obtained value of $\langle \hbar\omega \rangle$ for phonons, we see that $\langle \hbar\omega \rangle \gg kT$. This means that $E_G(T) \cong E_g(0)$. So, according to this theory, energy gap in QW should be independent of temperature for the range of temperature in our experiment. This is however, not justified from our experiment. So, we conclude that Varshni equation gives a better explanation to the temperature dependence of band gap.

Electron-phonon coupling: At low temperature, thermal inter band excitations are negligible. As the temperature increases, more electrons enter valance band. Also, lattice phonons who have relatively small energies get excited in large number as the temperature increases. This influences the electron-phonon coupling [7].
Theoretical evaluation of electron-phonon coupling requires really complicated methods. Therefore, fitting equations and models (like the one mentioned above) are often use to parametrise this.
It has been shown that the lattice parameter too has same analytic form as electron-phonon coupling [7].

4.5 Challenges

As mentioned in previous chapter, instrument set up is very important. While performing the experiment, we had to face with two major challenges. First challenge was to make the light—emitted by the sample—fall on the entrance slit of monochromator and entrance of PMT successively and to avoid any source of white light from falling onto PMT as PMT is very sensitive to incoming light. This could be achieved by maintaining minimal background light. Second major challenge was managing a perfect cable connection between PMT and lock in. During the experiment, initially it was observed that the laser peak intensity decreases with time as shown in figure 4.8(a), but after fixing the cable wire problem, no decrease in intensity was observed (figure 4.8(b)).

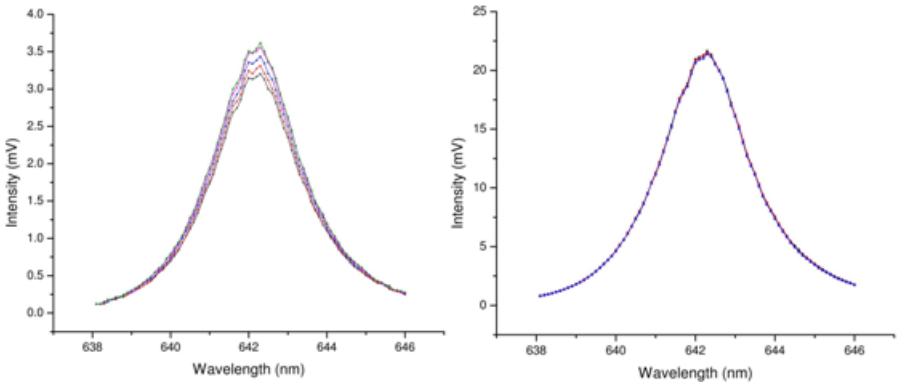

Figure 4.8: Laser intensity peak in (a) decreases as the measurement is repeated at a gap of 10 minutes (left), while in (b) it remains independent of time (right).

Chapter 5

Conclusion

This report deals with the main aim of the project —low temperature photoluminescence study of GaAs QW, detailed description of instrument set up for this experiment, obtained results and their analysis. Photoluminescence in semiconductors like GaAs depends mainly on two factors, namely laser excitation power and temperature. A higher laser power gives higher PL intensity, while increasing temperature causes decrease in intensity and redshift. Band gap too has a strong dependence on temperature. The experimental results obtained are well supported by theoretical and analytical approach. Instrument set up is a vital part of this experiment; with lock-in, PMT and monochromator having great importance and being widely used in experiments like this.

The next objective during this project was to study pholuminescence excitation (PLE) measurement, in which the detection energy for sample is kept fixed and excitation energy is varied (inverse to the case of PL study). But due to time limitation, this could only be a part of our future plan.

I thank Dr. Bipul Pal, Dr. Bhavtosh Bansal, Samrat Roy for their important contribution while carrying this project and IISER Kolkata for providing me a platform to carry this project.

Bibliography

[1] B. H. Bransden and C. J. Joachain, *Quantum mechanics*, 978-0-582-35691-7, Pearson, Harlow, 2000. 2nd edition, 515–527.

[2] J. R. Botha and A. W. R. Leitch, Journal of Electronic Materials 29, 12 (2000).

[3] S. L. Chuang, *Physics of Optoelectronic Devices*, 0-471-10939-8, Wiley, New York, 1995. 340–345.

[4] Y. Siegal, E. N. Glezer, L. Huang and E. Mazur, Annu. Rev. Mater. Sci. 25, 223–247 (1995).

[5] A. Chiari, M. Colocci *et al.*, Phys. Stat. Sol. (b) 147, 421 (1988).

[6] Y. P. Varshni, Physica 34, 149 (1967).

[7] K. P. O'Donnell and X. Chen, Applied Physics Letter 58, 2924 (1991).

[8] K. C. Chiu, Y. C. Su and H. A. Tu, Japanese journal of applied physics 37, 6374–6375 (1998).

[9] D. S. Jiang, H. Jung and K. Ploog, Journal of Applied Physics 64, 1371 (1988).

[10] P. Verma, G. Irmer and J. Monecke, J. Phys.: Condens. Matter 12, 1097–1110 (2000).

[11] Yu. I. Mazur, V. G. Dorogan *et al.* , Journal of Applied Physics 113, 144308 (2013).

[12] E. C. Le Ru, J. Fack, and R. Murray, PHYSICAL REVIEW B 67, 245318 (2003).

[13] Yutao Fang, Lu Wang *et al.*, Nature 5, 12718 (2015).

[14] L. Grenouillet, C. Bru-Chevallier *et al.*, Appl. Phys. Lett. 76, 2241 (2000).

[15] Atomic absorption spectroscopy learning module, retrieved from: https://blogs.maryville.edu/aas/wavelength-selection/.

[16] Hamamatsu, Photomultiplier tubes: Basics and applications, 3rd edition.

[17] About Lock-In Amplifiers, Application notes-3, Stanford research systems.

[18] Electronic Properties of Materials, MSE 5317. Retrieved from: http://electrons.wikidot.com/solar-cells.